

# Optical arbitrary waveform characterization via dual-quadrature spectral shearing interferometry

Houxun Miao<sup>1</sup>, Daniel E. Leaird,<sup>1,\*</sup> Carsten Langrock,<sup>2</sup> Martin M. Fejer,<sup>2</sup> and Andrew M. Weiner<sup>1</sup>

<sup>1</sup>*School of Electrical and Computer Engineering, Purdue University, West Lafayette, IN 47906, USA*

<sup>2</sup>*E. L. Ginzton Laboratory, Stanford University, Stanford, California 94305, USA*

\*Corresponding author: [leaird@purdue.edu](mailto:leaird@purdue.edu)

**Abstract:** We demonstrate a new dual-quadrature spectral shearing interferometry technique appropriate for spectral phase characterization of arbitrary optical waveforms generated by line-by-line shaping of high-repetition-rate (~10 GHz) optical frequency combs. Spectral shearing interferograms are generated through sum-frequency mixing of the frequency comb field with a pair of reference tones generated via intensity modulation of a continuous-wave laser. Although related to the well known SPIDER method, our approach relaxes spectral resolution requirements and operates in a collinear interaction geometry compatible with the use of high sensitivity, aperiodically poled lithium niobate nonlinear waveguide devices.

©2009 Optical Society of America

**OCIS codes:** (320.7100) Ultrafast measurements; (130.3730) Lithium niobate; (320.5540) Pulse shaping.

---

## References and links

1. Z. Jiang, D. S. Seo, D. E. Leaird, and A. M. Weiner, "Spectral line by line pulse shaping," *Opt. Lett.* **30**, 1557–1559 (2005).
2. Z. Jiang, C. B. Huang, D. E. Leaird, and A. M. Weiner, "Optical arbitrary waveform processing of more than 100 spectral comb lines," *Nature Photon.* **1**, 463–467 (2007).
3. R. P. Scott, N. K. Fontaine, J. Cao, K. Okamoto, B. H. Kolner, J. P. Heritage, and S. J. B. Yoo, "High-fidelity line-by-line optical waveform generation and complete characterization using FROG," *Opt. Express* **15**, 9977–9988 (2007).
4. D. Miyamoto, K. Mandai, T. Kurokawa, S. Takeda, T. Shioda, and H. Tsuda, "Waveform-Controllable Optical Pulse Generation Using an Optical Pulse Synthesizer," *IEEE Photon. Technol. Lett.* **18**, 721–723 (2006).
5. K. Takiguchi, K. Okamoto, T. Kominato, H. Takahashi, and T. Shibata, "Flexible pulse waveform generation using silica-waveguide-based spectrum synthesis circuit," *Electron. Lett.* **40**, 537–538 (2004).
6. D. J. Kane and R. Trebino, "Characterization of arbitrary femtosecond pulses using frequency-resolved optical gating," *IEEE J. Quantum Electron.* **29**, 571–579 (1993).
7. R. Trebino, *Frequency-resolved optical gating: the measurement of ultrashort laser pulses* (Kluwer Academic Publishers 2000).
8. C. Iaconis and I. A. Walmsley, "Spectral phase interferometry for direct electric-field reconstruction of ultrashort optical pulses," *Opt. Lett.* **23**, 792–794 (1998).
9. C. Iaconis and I. A. Walmsley, "Self-referencing spectral interferometry for measuring ultrashort optical pulses," *IEEE J. Quantum Electron.* **35**, 501–509 (1999).
10. Z. Jiang, D. E. Leaird, and A. M. Weiner, "Optical Arbitrary Waveform Generation and Characterization Using Spectral Line-by-Line Control," *J. Lightwave Technol.* **24**, 2487–2494 (2006).
11. V. R. Supradeepa, D. E. Leaird, and A. M. Weiner, "Optical Arbitrary Waveform Characterization via Dual-Quadrature Spectral Interferometry," *Opt. Express* **17**, 25–33 (2009).
12. L. Lepetit, G. Cheriaux, and M. Joffe, "Linear techniques of phase measurement by femtosecond spectral interferometry for applications in spectroscopy," *J. Opt. Soc. Am. B* **12**, 2467–2474 (1995).
13. H. Miao, S.-D. Yang, C. Langrock, R. V. Rostislav, M. M. Fejer, and A. M. Weiner, "Ultralow-power second-harmonic generation frequency-resolved optical gating using aperiodically poled lithium niobate waveguides," *J. Opt. Soc. Am. B* **25**, A41–A53 (2008).

14. C. B. Huang, S. G. Park, D. E. Leaird, and A. M. Weiner, "Nonlinearly Broadened Phase-Modulated Continuous-Wave Laser Frequency Combs Characterized using DPSK Decoding," *Opt. Express* **16**, 2520-2527 (2008).
15. C. Langrock and M. M. Fejer, "Background-free collinear autocorrelation and frequency-resolved optical gating using mode multiplexing and demultiplexing in reverse-proton-exchange aperiodically poled lithium niobate waveguides," *Opt. Lett.* **32**, 2306-2308 (2007).

## 1. Introduction

Optical arbitrary waveform generation (OAWG), in which pulse shaping is used to manipulate optical frequency combs on a line-by-line basis [1-5], leads to new challenges in waveform characterization. Fields generated through line-by-line pulse shaping exhibit several unique attributes. Such fields may exhibit 100%-duty cycle, with shaped waveforms spanning the full time-domain repetition period of the frequency comb, and with spectral amplitude and phase changing abruptly from line-to-line. OAWG fields are also characterized by large time-bandwidth product, approximately equal to the number of lines in the shaped frequency comb. Although methods for full characterization of ultrashort pulse fields, such as frequency-resolved optical gating (FROG) and spectral-phase interferometry for direct electrical field reconstruction (SPIDER), are well developed, e.g., [6-9], such methods are typically applied to measurement of low-duty cycle pulses that are isolated in time, have smoothly varying spectra and relatively low time-bandwidth product. These methods only require a low spectral resolution, and are therefore incompatible with the rapid spectral changes that are a hallmark of line-by-line pulse shaping.

Efforts towards waveform characterization for OAWG have been reported. For example, in [10] spectral phase was measured by observing the phase of the radio-frequency (RF) beat signal obtained when a line-by-line shaper was used to select two adjacent comb lines at a time from a 10-GHz frequency comb. In [3] signals from a 20 GHz optical comb were characterized by an X-FROG [7] technique in which the sum-frequency signal generated through the interaction of shaped and unshaped fields was spectrally resolved and measured as a function of delay. In [11] dual-quadrature spectral interferometry [12] was adapted for the measurement of 10-GHz repetition-rate OAWG waveforms. However, the techniques reported in [10] and [3] require a series of measurements performed sequentially, which slows down the measurement time, while the methods in [3] and [11] further require the availability of both unshaped and shaped fields.

In this paper we report a new self-referencing spectral shearing interferometry technique for full spectral-phase characterization of arbitrarily shaped optical frequency combs with an ~10-GHz repetition rate ( $f_{\text{rep}}$ ). Although our approach is related to SPIDER [9], which is also a spectral shearing interferometry method, it is modified in a number of important ways that optimize its applicability to frequency comb and OAWG waveforms. The differences between our technique and traditional SPIDER include the following:

1) In SPIDER a frequency shear is obtained via sum-frequency generation (SFG) of a pair of delayed (nonoverlapping) replicas of the pulse to be measured with a long chirp waveform (also derived from the pulse to be measured). In contrast, in the current spectral shearing interferometry approach, the frequency shear is obtained via SFG of the shaped comb field with a pair of reference tones.

2) SPIDER obtains spectral phase from the quantity  $\text{Re}\{E(\omega)E^*(\omega - \delta\omega)e^{j\omega\tau}\}$ , where  $\text{Re}$  is the real part,  $\delta\omega$  is the spectral shear, and  $\tau$  is the time delay. The current approach extracts the spectral phase from both quadratures of the quantity  $E(\omega)E^*(\omega - \delta\omega)$ .

3) SPIDER is appropriate for low-duty cycle sources and relatively short pulse widths, for which a pair of pulses can easily be separated in time. However, for waveforms with long time apertures, the delay requirement translates into difficult demands on spectral resolution (e.g., ~1 GHz for a 10 GHz comb source). In fact, from a fundamental perspective, for a periodic waveform with a 100%-duty cycle, it is impossible to achieve time separation greater than the temporal aperture of the waveform since the delay will also be periodic at the

repetition rate. In contrast, our zero-delay design relaxes spectral resolution requirements ( $\sim 5$  GHz for a 10 GHz comb) and is compatible with 100%-duty cycle OAWG sources.

4) Most SPIDER approaches utilize a second-harmonic or sum-frequency interaction to generate spectrally sheared waveform replicas. Unwanted self-terms from the nonlinear interaction are suppressed using a noncollinear geometry or by using Type-II phase matching [9]. In our approach the shaped field interacts with a pair of reference tones detuned in wavelength by more than the bandwidth of the shaped field. Therefore, the sheared waveform replicas are generated at a different wavelength than the unwanted self-terms, which can be separated using a spectrometer. As a result our experiment becomes compatible with a collinear waveguide interaction geometry. This enables the use of aperiodically poled lithium niobate (A-PPLN) waveguides for the sum-frequency generation step, which provides very good measurement sensitivity. Such A-PPLN waveguides have previously been exploited for characterization of low-duty-cycle ultrashort pulses via autocorrelation and FROG at average powers as low as nanowatts [13], but to our knowledge have not previously been applied in spectral shearing interferometry.

## 2. Measurement principle

Our approach obtains spectral shearing interferograms through the sum-frequency generation (SFG) of a signal field derived from an optical frequency comb source and a probe field consisting of a pair of single-frequency tones spaced at the comb repetition frequency. The different quadratures of the spectral shearing interferogram are accessed by modifying the relative phase between the two comb lines constituting the probe. We refer to this approach as dual-quadrature spectral shearing interferometry (DQ-SSI).

The measurement principle is as follows. We use

$$E_s(t)e^{i\omega_s t} \quad \text{and} \quad e^{i\phi_1} e^{i\omega_c t} + e^{i\phi_2} e^{i(\omega_c + \Omega)t} \quad (1)$$

( $\phi_1$  and  $\phi_2$  are unknown constant phase terms) to denote the time-domain signal and probe electric fields, respectively. The frequency separation  $\Omega$  between the two probe tones is equal to the frequency spacing between the comb lines of the signal field. Assuming a sufficiently broad phase matching bandwidth, the SFG signal resulting from the interaction of signal and probe fields is given by,

$$E_{SFG}(t) \propto E_s(t) e^{i\omega_s t} \left( e^{i\phi_1} e^{i\omega_c t} + e^{i\phi_2} e^{i(\omega_c + \Omega)t} \right) \quad (2)$$

Here we have neglected to write the (self) second-harmonic terms centered around the frequencies  $2\omega_s$  and  $2\omega_c + \Omega$ , respectively. These terms can be made to occur in frequency bands that are nonoverlapping with the SFG field and may therefore be discarded. The power spectrum of the SFG field may be written as

$$\begin{aligned} S_{SFG}(\omega) \propto & \left| \tilde{E}_s(\omega - (\omega_s + \omega_c)) \right|^2 + \left| \tilde{E}_s(\omega - (\omega_s + \omega_c + \Omega)) \right|^2 \\ & + 2 \left| \tilde{E}_s(\omega - (\omega_s + \omega_c)) \right| \left| \tilde{E}_s(\omega - (\omega_s + \omega_c + \Omega)) \right| \\ & \times \cos(\psi(\omega - (\omega_s + \omega_c)) - \psi(\omega - (\omega_s + \omega_c + \Omega)) + \phi_1 - \phi_2) \end{aligned} \quad (3)$$

where  $\tilde{E}_s(\omega)$  is the Fourier transform of  $E_s(t)$  and  $\psi(\omega)$  is the spectral phase, i.e., the phase of  $\tilde{E}_s(\omega)$ . The first two terms on the right side of Eq. (2) are background terms that do not provide spectral-phase information, while the third term provides information on the spectral-phase difference,  $\psi(\omega - (\omega_s + \omega_c)) - \psi(\omega - (\omega_s + \omega_c + \Omega))$ . The spectral-phase difference can be obtained by measuring the interferograms of Eq. (2) for a few different settings of the relative phase  $\phi_1 - \phi_2$  of the probe tones. In our experiments we perform four measurements, with the relative phase set in turn to 0,  $\pi/2$ ,  $\pi$ , and  $3\pi/2$  (relative to the initial setting, which need not be known). In this way we acquire in turn the cosine, negative sine, negative cosine, and sine dependencies of the third term, while keeping the background terms

unchanged. Thus one can completely retrieve the spectral phase of the signal. By subtracting the negative cosine interferogram from the cosine interferogram, we remove the background terms and isolate the third term in a form proportional to the cosine of the spectral phase difference. Similarly, by subtracting the negative sine interferogram from the sine interferogram, we isolate the third term in a form proportional to the sine of the spectral phase difference. Using these two results together, we easily retrieve the spectral phase difference. This procedure is unaffected by variations in the phase matching spectrum of the nonlinear crystal used for SFG, provided that the phase matching bandwidth is sufficient to encompass the full spectrum of the signal field. As in SPIDER, once the spectral phase difference is known, it is straightforward to recover the actual spectral phase function (up to the undetermined absolute phase).

A few remarks are in order. First, although here we recover the spectral phase from a sequence of four measurements, only three measurements are required. For example, one can calculate the background terms from the cosine and negative cosine terms (0 and  $\pi$  relative phase settings), then subtract the background from the  $3\pi/2$  measurement to obtain the term giving the sine of the spectral phase difference. In this way the  $\pi/2$  measurement is not needed. Second, the constant phase  $\phi_1 - \phi_2$  leads to an additional linear term in the spectral phase of the frequency comb under detection, which corresponds to a pure delay in the time domain. In many common pulse measurement techniques, e.g., FROG and SPIDER, the linear spectral phase and hence the delay cannot be obtained. However, in our dual-quadrature spectral shearing interferometry technique, the pair of probe tones produces an intensity beat in the time domain, whose temporal phase is determined by the value of  $\phi_1 - \phi_2$ . Therefore, the timing of the signal field relative to probe intensity beat signal can be extracted without ambiguity. Finally, for this paper we performed an auxiliary measurement of the power spectrum in order to obtain full signal field information. It should also be possible to derive the power spectrum directly from the DQ-SSI data, provided however that precise knowledge of the phase-matching spectrum of the A-PPLN is available.

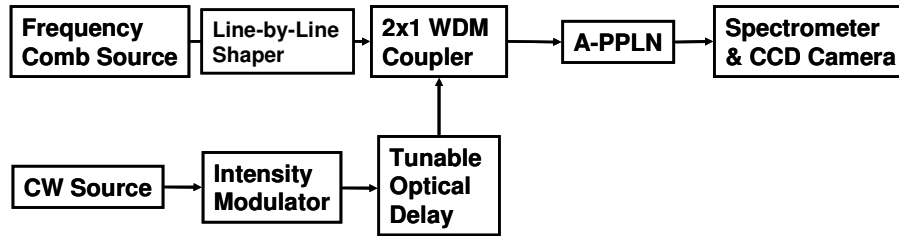


Fig. 1. Experimental setup.

### 3. Experimental setup

Figure 1 shows the experimental setup. For the signal field we start with a continuous-wave (CW) laser at 1542 nm with specified linewidth of 1 kHz, which is strongly phase modulated to produce a comb. The phase modulator, which is driven at an RF frequency equal to twice 9.953 GHz, is followed by an intensity modulator driven at 9.953 GHz [14]. This leads to a comb consisting of greater than thirty discrete lines spaced by the repetition rate  $f_{\text{rep}} = 9.953$  GHz. At this point the signal exhibits a strong spectral phase modulation and is spread in time over the full comb repetition period. The phase-modulated CW laser is followed by a line-by-line pulse shaper [2], which is used to block a few of the weaker lines at the edges of the spectrum and which is also used in later experiments to correct the spectral phase. After the line-by-line shaper, the signal consists of 28 comb lines, with a power spectrum as measured by an optical spectrum analyzer with a 0.01 nm spectral resolution shown in Fig. 2(a).

The probe field is derived from a second CW laser with  $\sim 1550$  nm wavelength, which is modulated by an integrated intensity modulator driven at  $(1/2)f_{\text{rep}}$ . The drive signal for the intensity modulator is obtained by splitting off a portion of the radio frequency (RF) signal

used to drive the signal field phase modulators, which is then launched into an RF divider ( $\div 2$ ) and an RF amplifier (10 dB). By adjusting the bias voltage of the intensity modulator for carrier suppression, we obtain a pair of comb lines (upper and lower modulation sidebands) separated by  $f_{\text{rep}}=9.953$  GHz and centered at the 1550 nm CW wavelength. The carrier-suppression ratio is  $\sim 20$  dB, as shown in the optical spectrum analyzer measurement of Fig. 2(b). We use a tunable optical delay line to set the delay of the probe field sequentially to 0, 25.1, 50.2, and 75.4 ps ( $0, 0.25/f_{\text{rep}}, 0.5/f_{\text{rep}},$  and  $0.75/f_{\text{rep}}$ ) relative to the signal field. For a probe field consisting of two optical tones, this is equivalent to cycling the relative optical phase  $\phi_1 - \phi_2$  through the values  $0, \pi/2, \pi,$  and  $3\pi/2$ .

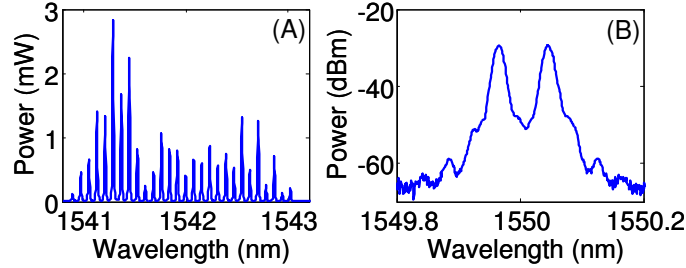


Fig. 2. Spectra of the signal comb (a), and the probe field (b).

The signal and the probe are combined together with a 3-dB coupler and launched into an apodized aperiodically poled lithium niobate (apodized A-PPLN) waveguide [15]. The A-PPLN waveguide is fiber coupled at the input side and used at room temperature, where its phase matching spectrum is 50 nm wide and centered at 1538 nm. The sum-frequency generation field is coupled from the A-PPLN waveguide directly into free space. It then passes through a home-made 30X beam expander and spectrometer (1800 line/mm grating, 75 cm focal length lens) and is focused on a non-intensified CCD camera. The CCD pixels are spaced by 16  $\mu\text{m}$ , and the sum-frequency spectrum is dispersed by 3.3 GHz per pixel, corresponding to 3 pixels per comb line. The crosstalk from a spectral line three camera pixels away was less than 10%. DQ-SSI measurements were performed with average signal and probe powers of  $\sim 400$   $\mu\text{W}$  and  $\sim 160$   $\mu\text{W}$ , respectively, and a detector integration time of 5.28 ms.

#### 4. Experimental results

We first measured the spectral phase of the modulated CW comb source with the pulse shaper programmed to be inactive. Figure 3(a) shows the data for delay at the zero setting. With our choice of signal and probe wavelengths, the sum frequency spectrum ( $\sim 773$  nm) corresponding to the interaction of signal and probe fields is clearly separated from the second-harmonic signals of either the signal field ( $\sim 771$  nm) or probe field ( $\sim 775$  nm) acting alone. Of these, only the spectrum corresponding to the interaction of signal and probe fields constitutes an interferogram that varies with delay and can be used to extract the spectral phase. Although not implemented here, note that a narrower A-PPLN phase-matching spectrum can be selected in order to suppress the unnecessary second-harmonic generation background terms. Figures 3(b)-3(e) show the four spectral shearing interferograms obtained with the optical delays (equivalent to the relative phase of the probe tones) set as specified above. Figure 4(a) shows the retrieved spectral phase, which as expected shows strong variation from line-to-line. Figure 4(b) shows one period of the temporal intensity profile calculated from the retrieved spectral phase and the previously measured power spectrum (Fig. 2(a)). Although the calculated intensity shows variations, the waveform is clearly spread over much of the full repetition period, as expected for a comb generated predominantly via phase modulation of a CW laser.

Repeatability is an important aspect of any measurement technique. To check the repeatability of our technique, we performed 10 independent DQ-SSI measurements of the comb source prior to phase correction. The residuals of the ten measurements (i.e., the

difference of each measurement point from the mean for that spectral line) are overlaid in Fig. 5(a). The residuals are mostly within  $\pm 0.1$  rad. Figure 5(b) shows the standard deviations of the measured spectral phases for each individual comb line. The average standard deviation is 0.039 rad, while even the worst case standard deviation is only 0.076 rad. These findings indicate excellent repeatability.

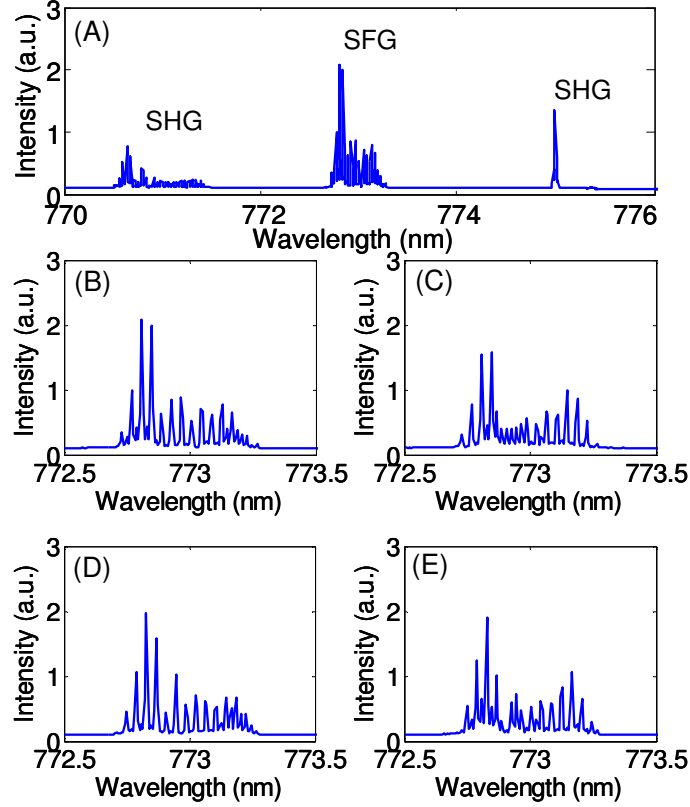


Fig. 3. Spectral shearing interferograms. (a) The full camera window at zero delay. (b-e) Zoom-in to the SFG term for four delays of 0, 25.1, 50.2, and 75.4 ps.

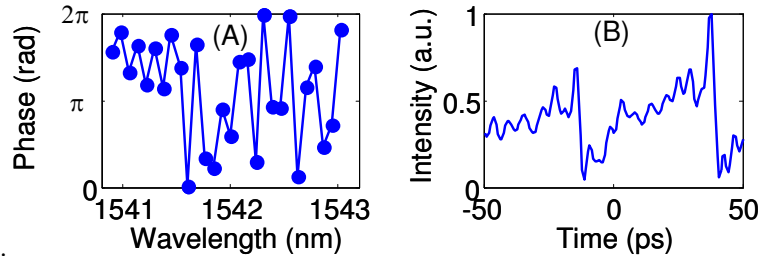


Fig. 4. Retrieved spectral phase (a) and the calculated temporal intensity profile (b) of the pulse under detection. The spectral phase of adjacent comb lines are connected by lines.

We validated the measurement results in several ways. In a first method, we flattened the spectral phase by using the line-by-line pulse shaper to apply the inverse of the measured spectral phase. We then repeated our measurement of the optical frequency comb. Figures 6(a) and 6(c) show the spectrum measured via OSA and the retrieved spectral phase, respectively. Despite the finite spectral resolution of the pulse shaper, which introduces some slight intensity modulation during the phase correction operation, the power spectrum remains quite similar to that shown in Fig. 2. Most importantly, the measurement indeed indicates flat

spectral phase: the mean of the spectral phase over 28 comb lines is near zero, with a standard deviation of only 0.092 rad. Figure 6(b) shows the calculated temporal intensity profiles of the comb both with the measured spectral phase and with an ideal flat spectral phase. Figure 6(d) shows the same intensity profiles, but zoomed in on the delay axis. The curves are essentially indistinguishable, which further confirms that after spectral phase correction, the pulse is close to bandwidth limited.

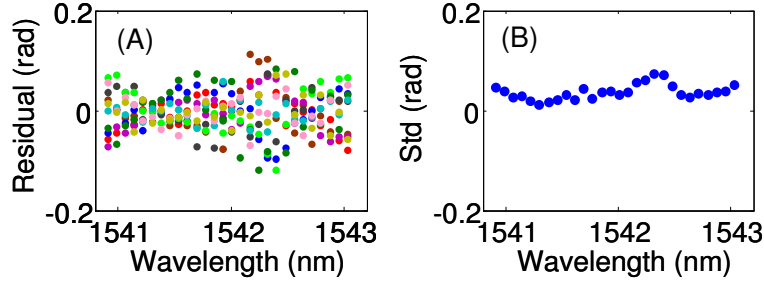


Fig. 5. (a) Residuals of ten independent DQ-SSI measurements. (b) Standard deviation of the measured spectral phase of each comb line.

As a second validation method, we measured the intensity autocorrelation trace of the initial comb source and compared it to the autocorrelation trace calculated on the basis of the measured spectrum and the retrieved spectral phase of Fig. 4. Figure 7(a) shows measured and calculated autocorrelation traces. The two traces are in close agreement. To further confirm the accuracy of the spectral phase measurement, we measured the autocorrelation trace of the comb source after spectral phase correction and compared it to the theoretical autocorrelation calculated assuming flat spectral phase. Figure 7(b) shows the results. Again the traces are essentially indistinguishable. These results show that after phase correction, the pulse is very close to bandwidth limited, which is consistent with the results shown in Fig. 6. Because the phase correction is based solely on the spectral phase retrieved prior to correction, this demonstrates convincingly that the retrieved phase is accurate.

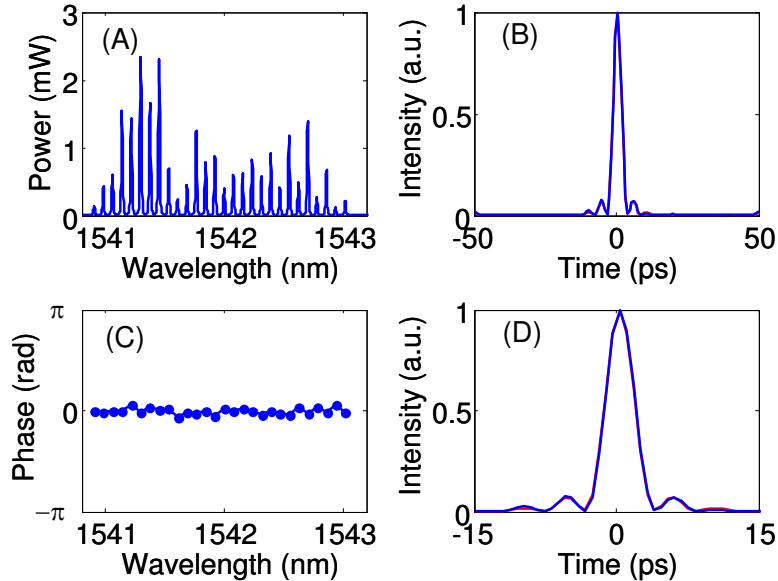


Fig. 6. (a) Measured spectrum of the optical frequency comb after compensating the phase to generate a short pulse. (b&d) Calculated temporal intensity profile with measured spectral phase (blue) and ideal flat spectral phase (red). (c) Measured spectral phase.

For further validation we compared the spectral phase retrieved for the uncompressed comb using DQ-SSI with the spectral phase obtained via an independent method. In this independent method our procedure involved programming the line-by-line shaper to add one comb line at a time (starting with three) and adjusting the phase of the new frequency component (with step sizes of  $\pi/12$ ) in order to maximize the second-harmonic generation signal from an autocorrelator set at zero delay [14]. The result of the comparison is shown in Fig. 8, with the DQ-SSI data in blue and the data from the independent method in red. The two measurements are clearly very similar, with differences not much larger than the  $\pi/12$  discretization of the independent method.

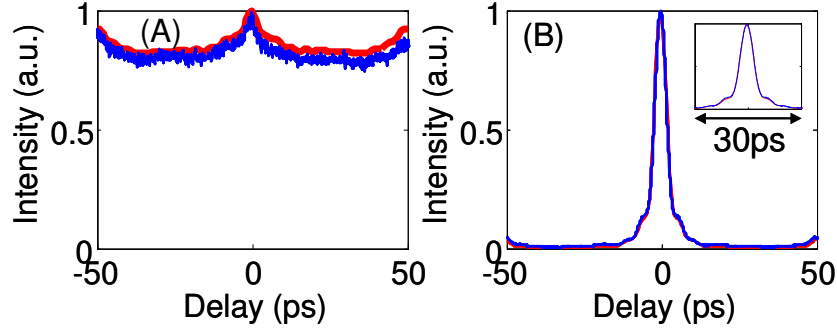


Fig. 7. (a) Measured (blue), and calculated (red) autocorrelation before phase compensation. (b) Measured (blue) and calculated (red) autocorrelation after phase compensation.

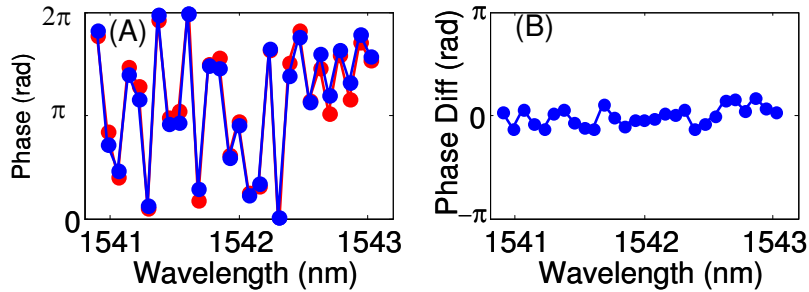


Fig. 8. (a) Phase retrieved from DQ-SSI method (blue), and an independent measurement method (red). (b) Phase difference between the two methods on a spectral line-by-line basis.

Finally, we performed a measurement for a shaped pulse. Here the line-by-line pulse shaper was programmed for cubic spectral phase (cubic phase is applied in superposition with the phase needed for compression, as per Fig. 4). The results are shown in Fig. 9. Figure 9(a) compares the phase obtained from DQ-SSI (blue) with the target phase applied to the pulse shaper (cubic part only, red). Figure 9(b) shows the difference between the two data sets in Fig. 9(a) on a line-by-line basis. The excellent agreement evident in Fig. 9 further confirms the accuracy of our new dual-quadrature spectral shearing interferometry phase measurement technique.



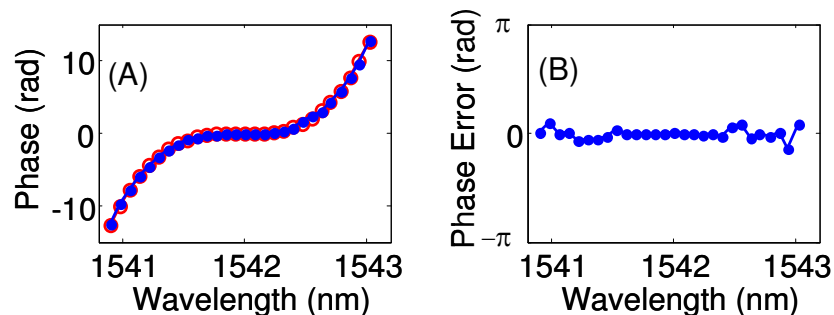


Fig. 9. Measurement of a shaped pulse. (a) Phase retrieved from the DQ-SSI method (blue), and target phase applied to the shaper (red). (b) Phase difference between the two data sets in (a) on a spectral line-by-line basis.

## 5. Conclusion

We have demonstrated a new method for spectral phase characterization of optical arbitrary waveforms generated via line-by-line shaping of high repetition rate frequency comb fields. Our dual-quadrature spectral shearing interferometry approach, although similar to the well known SPIDER measurement technique, is adapted to match unique waveform characteristics. Our zero delay design relaxes spectral resolution requirements and is compatible with the 100%-duty cycle fields characteristic of line-by-line pulse shaping. Furthermore, our sum-frequency generation scheme allows wavelength separation of desired spectral shearing terms from unwanted second-harmonic generation background terms. This makes it possible to perform spectral shearing interferometry measurements in a collinear geometry compatible with the use of highly efficient A-PPLN waveguide nonlinear crystals, which offers potential for operation at low optical power.

## Acknowledgments

This work was supported by DARPA/ARO under grant W911NF-07-1-0625 and by NSF under grant ECCS-0601692. We thank C.-B. Huang and F. Ferdous for assistance with the frequency comb source and R.V. Roussev for contributions to the A-PPLN nonlinear waveguides.